Minerals Engineering 66–68 (2014) 197–201

Contents lists available at ScienceDirect

Minerals Engineering

journal homepage: www.elsevier.com/locate/mineng

Pyrite recovery mechanisms in rougher flotation circuits

J. Yianatos *, C. Carrasco [1], L. Vinnett, I. Rojas

Automation and Supervision Centre for Mining Industry, CASIM, Department of Chemical and Environmental Engineering, Federico Santa Maria Technical University, Chile

ARTICLE INFO

Article history:
Received 26 December 2013
Revised 18 March 2014
Accepted 21 March 2014
Available online 13 April 2014

Keywords:
Pyrite flotation
Entrainment
Bubble load
True flotation

ABSTRACT

Bubble load and top of froth measurements per size class were carried out in a rougher flotation circuit containing sulphide copper minerals and pyrite. This circuit consists of four parallel banks of seven 130 m^3 mechanical cells. Results of testing the first rougher cell (approximately 69% Cu recovery), showed that 40–60% of pyrite in the finer class of the concentrate (−45 μm) was recovered by entrainment. For the coarser classes, pyrite was preferentially recovered to the concentrate by true flotation or association. These results were validated by batch flotation tests, using the same feed material to the rougher flotation circuit.

The bubble load and top of froth measurements permitted the evaluation of the pyrite transport mechanisms at industrial scale, providing estimations of pyrite true flotation and entrainment which are relevant for pyrite depression evaluation.

1. Introduction

Non-valuable iron sulphides are often associated with valuable sulphide minerals. These iron sulphides are of critical importance in Cu/Mo flotation concentrators because of their impact on product quality (concentrate grade) and efficiency (mineral recovery). For instance, it is well-known that the difficulties in separating valuable species such as chalcopyrite from pyrite lead to a significant decrease of the concentrate Cu grade.

Several works (Bushell and Krauss, 1962; Weisener and Gerson, 2000; Voigt et al., 2004; Peng et al., 2003a, 2003b) have discussed the impact of grinding media conditions on the flotation of pyrite and valuable minerals. It has been stated that pyrite presents poor floatability in alkaline conditions mainly because of the dominant effect of oxidized iron species from the grinding media depressing the pyrite (Peng et al., 2003a). However, surface reactions and electrochemical processes might promote pyrite activation, which is pointed out as the main reason for pyrite flotability. Those surface reactions might lead to adsorption of copper ions from solution onto other minerals such as pyrite (Weisener and Gerson, 2000), where the copper ions act as sites for collector adsorption. Peng and Grano (2010) suggested that the activation of pyrite by Cu^{2+} involves the reduction of copper (II) to copper (I) and the formation of a new metal sulphide phase, in which the xanthate adsorption is similar to the adsorption of Cu sulphide minerals.

In various works, pyrite flotation has been studied at the pilot and industrial scale. Kawatra and Eisele (1997) suggested that flotation of liberated pyrite in coal cleaning plants was not an important recovery mechanism compared to entrainment and mechanical locking with floatable particles. Trahar et al. (1994) indicated that under alkaline conditions, the recovery of pyrite is dominated by entrainment. Nevertheless, interactions between sulphide minerals might promote pyrite floatability. Vera et al. (1999) reported kinetic rate constants for chalcopyrite and pyrite in a 16L pilot flotation cell under different operating conditions. More recently, Dobby and Savassi (2005) considered pyrite as a floatable species based on batch flotation test results.

In this work, the pyrite recovery mechanisms in a Cu/Mo rougher flotation bank were studied based on bubble load and top of froth measurements. The industrial results were corroborated by means of flotation batch tests.

2. Experimental procedure

Mass balances were carried out in parallel with bubble load measurements in order to determine the pyrite recovery to the concentrate by entrainment or collection processes (true flotation or association). Metallurgical datasets were analysed and reconciled per size class. In addition, the pyrite transported to the concentrate stream in the rougher circuit was evaluated from top-of-froth (TOF) measurements. TOF grades have shown a high correlation with bubble load grades in non-selective froths (Yianatos and Contreras, 2010). In addition, the TOF measurements are suitable in evaluating the collection process down the flotation bank, due to the larger

* Corresponding author. Address: P.O. Box 110-V, Valparaíso, Chile. Fax: +56 32 654478.
E-mail address: juan.yianatos@usm.cl (J. Yianatos).
[1] Present Address: University of Queensland, Australia.

http://dx.doi.org/10.1016/j.mineng.2014.03.020
0892-6875/

sample sizes possible (regarding the bubble load). The results obtained along the rougher circuit were verified by laboratory batch tests. The following section describes the experimental procedure.

2.1. Plant conditions and mass balance adjustment

A metallurgical characterisation of a collective Cu/Mo rougher flotation bank was performed. The rougher circuit consists of four parallel banks of seven 130 m^3 mechanical cells, in a 1–2–2–2 arrangement as shown in Fig. 1. Sampling points in first, second, third and overall rougher bank are shown.

Three sampling campaigns were carried out in order to determine the pyrite recovery along the rougher banks. Grade data were adjusted to satisfy the total and component mass balances. Chemical assays by elements (Cu, Mo, Fe and insoluble) were conducted and samples were classified per size class (+150 μm, −150 μm, +45 μm and −45 μm). Table 1 shows the operating conditions of the rougher circuit during the surveys. Survey 2 was accomplished under typical operating conditions. Surveys 1 and 3 were carried out to support this study.

An example of reconciled grade data per size class is shown in Table 2 for Cu and Fe around the first rougher cell during Survey 2. In each survey the fine class corresponded to approximately 50% of the overall rougher feed. The Fe feed grade in the three sampling campaigns was in the range of 4.4–4.6%.

Based on the mineral distribution observed in the grinding circuit, it was found that Cu was fed to the flotation circuit mainly as chalcopyrite (70%), bornite (18%) and digenite (11%) minerals, Mo as molybdenite (≈100%) and Fe as chalcopyrite (50%) and pyrite (47%). Notice that under these conditions, pyrite recovered to the concentrate stream can be estimated from the Cu grade data, assuming similar floatability of chalcopyrite, bornite and digenite.

2.2. Bubble load measurements

Bubble load was measured using the USM bubble load sensor. This device allows bubble load sampling just below the pulp–froth interface in order to calculate the actual mineral transport from the pulp to the froth by true flotation. Thus, using mass balances around a flotation cell along with bubble load results, the froth recovery and particle entrainment can be estimated (Yianatos and Contreras, 2010; Yianatos et al., 2008). The experimental procedure and data analysis for bubble load measurement have been previously described by Yianatos et al. (2008). Fig. 2 shows the apparatus used for bubble sampling in industrial flotation cells.

2.3. Top of froth measurements

The top-of-froth (TOF) sampler was used for sampling the first layer at the surface of the froth as described by Yianatos and Contreras (2010). The information provided by the TOF samples allows the description of grade and size distribution of the collected minerals which reach the concentrate after froth drainage and coalescence. Yianatos et al. (2008) concluded that the froth transport of collected minerals per size class was rather non-selective for shallow froths in Cu rougher flotation. Thus, under the aforementioned condition the TOF grade can be used to estimate the bubble load grade (Yianatos and Contreras, 2010).

Table 1
Plant conditions in the rougher flotation circuit during the metallurgical surveys.

	Survey 1	Survey 2	Survey 3
No of operating banks	2	4	3
Feed flowrate per bank, tph	479	726	708
Cu grade, %	0.84	1.01	0.96
Fe grade, %	4.46	4.47	4.58
Mo grade, %	0.02	0.02	0.02
Solid percentage, %	28	41	39
pH	9.5	9.4	9.5

2.4. Flotation batch tests

Flotation tests were conducted in order to identify the flotation rate of each mineral species at laboratory scale. Thus, the content of chalcopyrite, molybdenite and pyrite were estimated per size class. The samples were taken from the feed of the industrial flotation plant (Table 1).

The feed, final tail and concentrate samples were screened in three size classes (+150 μm, −150 μm, +45 μm and −45 μm). The concentrate was sampled at 1.5, 3, 6 and 12 min. intervals. Each size class was assayed for Cu, Mo, Fe and insolubles.

3. Results

3.1. Rougher flotation circuit

Table 3 summarizes the bubble load and TOF measurements along with the froth depth conditions, h_F. Bubble load measurements BL3, BL4 and BL6 (Table 3) were analysed using the cyclosizer system (Sepor Inc, 2013) in order to compare the particle size distribution of the collected material in the first rougher cell under typical operating conditions (Table 1).

Fig. 3 shows the particle size distribution of bubble load in the first rougher cell for samplings BL3, BL4 and BL6. It is observed that the particle size distribution of the collected material did not change significantly between Surveys 2 and 3, as shown in Table 1.

Fig. 4 shows a comparison of collected plus associated pyrite distributions per size class in the bubble load of the first rougher cell. These results were estimated from the mineralogical distribution of the Cu and Fe minerals in the raw feed, assuming similar

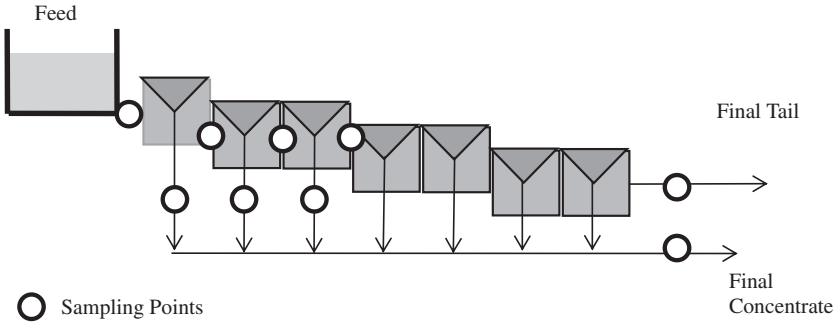

Fig. 1. Arrangement and sample points in the rougher flotation banks.

Table 2
Mass balance adjustment results around the first cell per size class (μm).

Stream	Total grades, %		Cu grades, %						Fe grades, %					
	Cu	Fe	−45 μm	+45 μm	−75 μm	+75 μm	−150 μm	+150 μm	−45 μm	+45 μm	−75 μm	+75 μm	−150 μm	+150 μm
Feed	1.01	4.47	1.20	1.44		0.86		0.51	5.11	4.66		3.87		3.43
Concentrate	5.38	8.40	4.57	8.47		7.06		6.75	7.10	12.71		11.98		10.02
Tail	0.36	3.89	0.39	0.34		0.30		0.35	4.63	3.42		3.14		3.27
Recovery, %	69.1	24.3	73.7	79.6		67.8		32.0	27.1	36.5		25.5		7.0

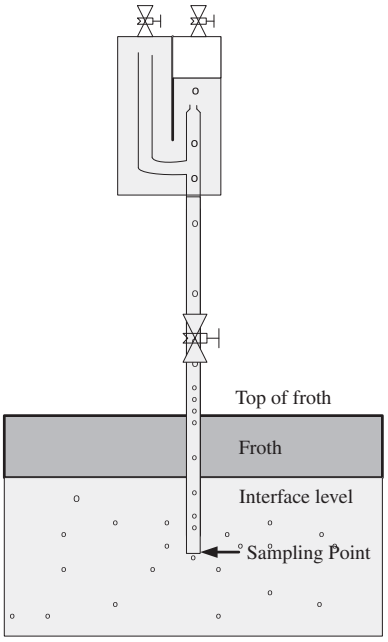

Fig. 2. Bubble load sensor (Yianatos et al., 2008).

Table 3
Bubble load and TOF sampling conditions.

Bubble load	Cell number	Survey	h_F, cm	Top-of-froth	Cell number	Survey	h_F, cm
BL1	1	1	3–5	TOF1	1	1	5
BL2	1	1	5	TOF2	1	2	5–7
BL3	1	2	4	TOF3	2	2	10–15
BL4	1	2	5–7	TOF4	3	2	15
BL5	2	2	10–15	TOF5	4	2	10
BL6	1	3	5	–	–	–	–

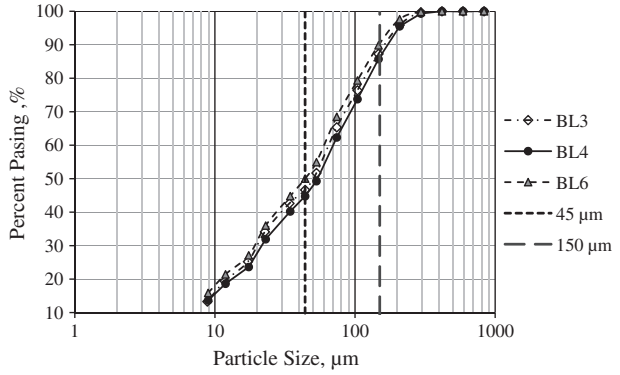

Fig. 3. Particle size distribution of bubble load.

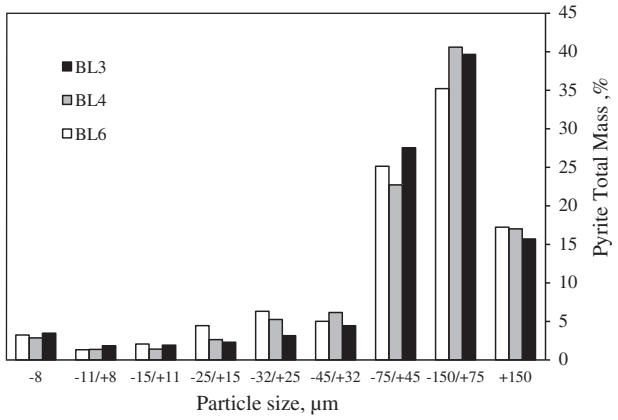

Fig. 4. Mass distribution of pyrite per size class in the bubble load samples.

floatability of the different valuable species. Notice that the pyrite distributions in the bubble load were similar in shape, with highest relative frequency between 45 μm and 150 μm.

To identify the pyrite flotation mechanisms, a comparison between the collected/associated pyrite in the bubble load and the pyrite recovered to the concentrate stream was carried out. The collected/associated minerals were determined from the bubble load measurements whereas the minerals in the concentrate stream were obtained from the mass balance adjustments. Fig. 5(a) and (b) shows the collected valuable (Cu minerals) and pyrite per size class in the bubble load and concentrate stream during Survey 2. In each class, Cu minerals in the bubble load were higher than in the concentrate stream, because some fraction of the floatable material returned from the froth to the collection zone due to coalescence or collapse of bubbles (froth dropback). Hence, Cu minerals were mainly recovered by true flotation assuming negligible entrainment of valuable solids (Yianatos et al., 2008). Under this condition, it was found the ratio between the valuable minerals flowrate in the concentrate stream and the valuable minerals flowrate in the bubble load corresponds to the froth recovery.

From the mass balances in the first rougher cell, the pyrite transported to the concentrate by entrainment ranged from 40% to 60% of the total pyrite recovered in the fine class. Fig. 5(b) shows that the fine pyrite flowrate recovered to the concentrate stream was significantly higher than the collected pyrite flowrate in the −45 μm class because of entrainment. On the other hand, the coarser classes of pyrite transported to the concentrate were either associated with valuable minerals or directly collected.

3.2. Pyrite floatability along the rougher bank

To characterise the pyrite floatability along the rougher flotation bank, TOF measurements were conducted in the first four mechanical cells. TOF and collected solid grades were expected to be similar, assuming non-selective froths. Fig. 6 shows the pyrite TOF grade down the bank. Notice that among the coarser classes, a

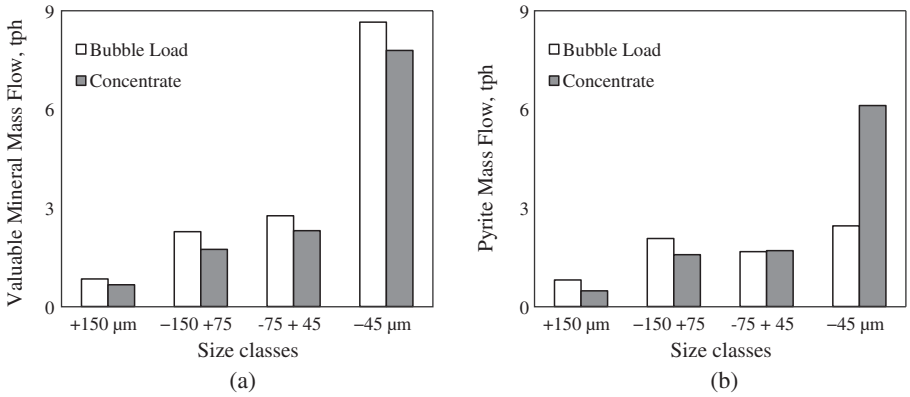

Fig. 5. Mass flowrates in bubble load and concentrate stream of (a) valuable (Cu minerals) and (b) pyrite, Survey 2.

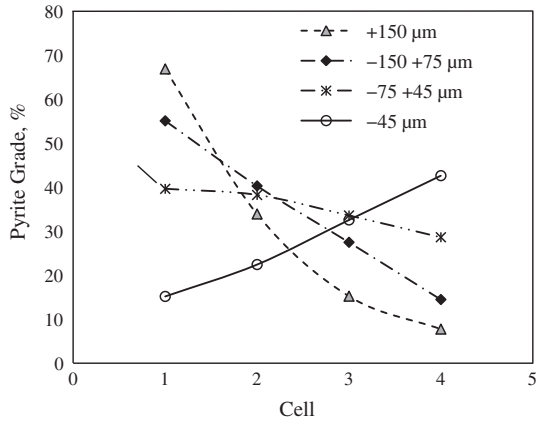

Fig. 6. Pyrite grade in top of froth along the rougher flotation bank.

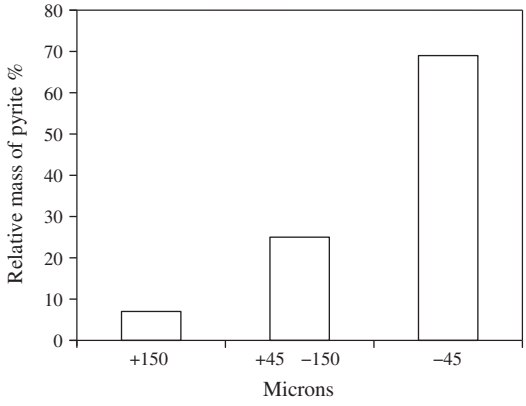

Fig. 8. Percentage of total mass of pyrite in concentrate.

decreasing TOF grade is observed, which suggests a collection process similar to those observed for valuable minerals. Thus, the pyrite recovery in the coarser classes was related to either association or true flotation (because of activation) along the rougher bank.

The pyrite TOF grade in the −45 μm size class showed an increase in the first four cells. A fraction of fine pyrite was also recovered by association or true flotation, possibly because the solid in this class was more liberated. The increase in the TOF grade was caused because of the strong decrease in the valuable solid concentration in the first cells and an apparently slower collection rate of pyrite, which, relative to a lesser collected mass, showed a higher pyrite grade down the bank. Thus, the mechanisms of fine pyrite recovery were a superposition of true flotation and entrainment as shown in Figs. 5 and 6.

3.3. Laboratory tests

Batch flotation tests of the rougher feed from Survey 2 were carried out in three size classes. Fig. 7(a) and (b) shows the kinetic response for both overall solid and solid per size class, respectively. It was found that in coarser classes, Fig. 7(b), the pyrite showed a

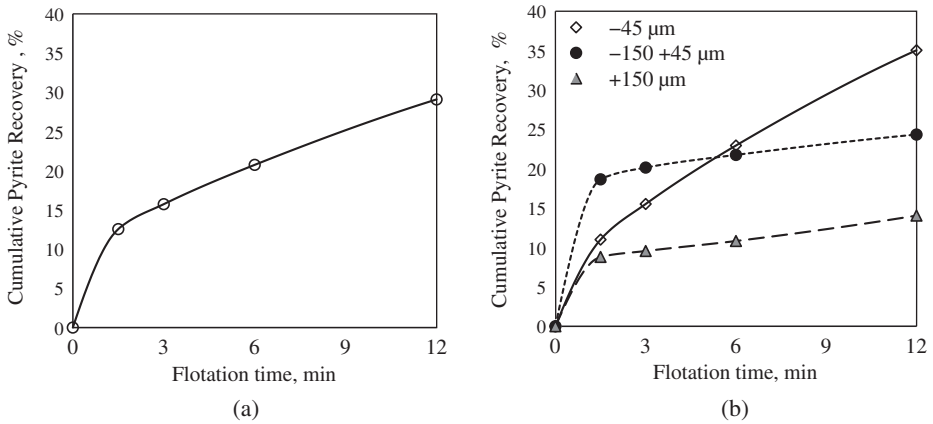

Fig. 7. Batch pyrite kinetics, Survey 2 (a) overall and (b) per size class.

kinetic response similar to those obtained from valuable solids, which confirmed that in these classes pyrite was recovered by association or true flotation. In the finer class, however, the kinetic response showed an increasing trend which was related to the significant impact of the pyrite entrainment on the fine pyrite recovery.

Fig. 8 shows the relative mass of pyrite recovered per size class in the concentrate. Notice that around 70% of the pyrite was recovered under −45 μm, which had a significant impact on the total pyrite recovery, as shown in Fig. 7(a).

Based on the industrial and laboratory results, the pyrite recovery in the finer class corresponds to the sum of pyrite entrainment (e.g., 40–60% in the first rougher cell) and pyrite recovered by true flotation. In the coarser classes, the pyrite was recovered rather by true flotation or association, which was observed at industrial and laboratory scale.

4. Conclusions

Using bubble load measurements along with mass balances at industrial scale (first rougher cell), it was observed that a range of 40–60% of pyrite under −45 μm was recovered in the concentrate by entrainment. From top of froth grade measurements along the rougher bank, it was observed that a fraction of fine pyrite was also recovered by true flotation (top of froth grade increasing), considering that the solids in this class were more liberated. On the other hand, the coarse pyrite (+45 μm) was mainly recovered to the concentrate by true flotation or association with valuable minerals as indicated by top of froth grade decreasing along the rougher bank. Also, the activation of pyrite in liberated particles may occur.

From batch tests, it was found that in the coarser classes the pyrite had a kinetic response similar to those of valuable solids, which confirmed that in coarser classes, pyrite was recovered by either association or true flotation. In the finer class, the kinetic response displayed an increasing trend which was related to the significant impact of the fine pyrite entrainment on pyrite recovery.

Acknowledgements

The authors are grateful to El Teniente Division Codelco-Chile and Carlos Torres for providing access to their plant and the valuable assistance in Cristian Carrasco's thesis development. Funding for process modelling and control research is provided by CONICYT, Project Fondecyt 1130568 and Federico Santa María Technical University, Project 271351.

References

Bushell, C., Krauss, C., 1962. Copper activation of pyrite. Can. Min. Metall. Bull. 55 (601), 314–318.
Dobby, G., Savassi, O., 2005. An Advanced Modelling Technique for Scale-up of Batch Flotation Results to Plant Metallurgical Performance. In: Jameson, En G. (Ed.), Centenary of Flotation Symposium. Centenary of Flotation Symposium, Bribasne, Australia, pp. 99–103.
Kawatra, S., Eisele, T., 1997. Pyrite recovery mechanisms in coal flotation. Int. J. Miner. Process. 50 (3), 187–201.
Peng, Y., Grano, S., 2010. Effect of grinding media on the activation of pyrite flotation. Miner. Eng. 23 (8), 600–605.
Peng, Y., Grano, S., Fornasiero, D., Ralston, J., 2003a. Control of grinding conditions in the flotation of chalcopyrite and its separation from pyrite. Int. J. Miner. Process. 69 (1–4), 87–100.
Peng, Y., Grano, S., Fornasiero, D., Ralston, J., 2003b. Control of grinding conditions in the flotation of galena and its separation from pyrite. Int. J. Miner. Process. 70 (1–4), 67–82.
Sepor Inc, 2013. Cyclosizer for Sub-sieve Sizing. Sepor Inc, Wilmington, CA.
Trahar, W., Senior, G., Shannon, L., 1994. Interactions between sulphide minerals – the collectorless flotation of pyrite. Int. J. Miner. Process. 40 (3–4), 287–321.
Vera, M., Franzidis, J., Manlapig, E., 1999. Simultaneous determination of collection zone rate constant and froth zone recovery in a mechanical flotation environment. Miner. Eng. 12 (10), 1163–1176.
Voigt, S., Szargan, R., Suoninen, E., 2004. Interaction of copper(II) ions with pyrite and its influence on ethyl xanthate adsorption. Surf. Interface Anal. 21 (8), 526–536.
Weisener, C., Gerson, A., 2000. Cu(II) adsorption mechanism on pyrite: an XAFS and XPS study. Surf. Interface Anal. 30, 454–458.
Yianatos, J., Contreras, F., 2010. Particle entrainment model for industrial flotation cells. Powder Technol. 197 (3), 260–267.
Yianatos, J., Moys, M.H., Contreras, F., Villanueva, A., 2008. Froth recovery of industrial flotation cells. Miner. Eng. 21 (12–14), 817–825.